ELSEVIER

Thermochimica Acta 2570 (1995) 743–753

thermochimica
acta

Thermal analysis as a method of characterizing ancient ceramic technologies ☆

A. Moropoulou [a,*], A. Bakolas [b], K. Bisbikou [a]

[a] *Department of Chemical Engineering, Section of Materials Science and Engineering, National Technical University of Athens, 9 Iroon Polytechniou, 15773 Athens, Greece*

[b] *Dipartimento di Scienze Ambientali, Universita di Venezia, 2137 Calle Larga S. Marta, 30123 Venezia, Italy*

Received 16 September 1994; accepted 9 June 1995

Abstract

Ceramic materials represent manufacturing techniques which were improved consistently during the course of time. The components of ceramic materials are the "fingerprint" of the stable and/or metastable solid phases formed during the firing; the production processes of antique ceramics and pottery can be derived from their assemblage. There are many recognizable phases and their association depends, more than on their chemistry, upon the mineralogy of the raw materials, their grain-size distribution, maximum heating temperature, heating ratio, duration of firing and kiln redox atmosphere. All these factors help in understanding the "course" of reactions.

Heating also affects the contact between the fine-sized clayey matrix and mineral clast fragments, appearing in reaction rims, sometimes showing newly-formed phases. The temperature at which ancient ceramics and pottery were fired varies over a wide range (600–1300°C) depending on the type of clay used and the kiln available, although firing temperatures not above 300–400°C have also been suggested.

Clay minerals, as the main material for production of ceramics and pottery, show some characteristic reactions (dehydroxylation, decomposition, transformation) in the course of firing (heating effects) and several thermoanalytical criteria can be used for reconstruction of former production conditions.

In the present work DTA, TGA and XRD results from byzantine and medieval ceramics are examined and information derived on ceramic technologies concerning raw materials and production conditions is validated by SEM observations concerning the extent of vitrification, as well as by the microstructural data provided by porosimetric measurements.

☆ Presented at the 6th European Symposium on Thermal Analysis and Calorimetry, Grado, Italy, 11–16 September 1994.

* Corresponding author.

SSDI 0040-6031(95)02570-7

Keywords: CaO transformation; Ceramic micro-fabric; Ceramic technology; Discriminant factors; Extent of vitrification; Firing temperature; Raw clays

1. Introduction

The characterization of archaeological ceramics and pottery can be improved by thermal analysis, especially as concerns firing temperatures and/or presence of raw (secondary) phases [1]. DTA curves enable detection of exo- and endothermic peaks (effects due to gain/loss of enthalpy) occurring in the sample when undergoing controlled heating and compared to an inert reference material. In clay minerals, the endothermic peak around 100°C is due to moisture water, whereas those appearing at about 200–250°C are attributed to "bound" water, or to "hydrated" interlayer cations (as in swelling clay minerals). Gypsum, if present, also shows endothermic effects within the range 120–160°C [2]. Iron hydroxides lose their water at about 300°C (endothermic peak), but this effect may be overlapped by an exothermic peak at 300–350°C due to the recrystallization of amorphous and/or ill-crystallized Fe-oxy hydroxides [1].

Also, organic matter (used as binder in the preparation of the ceramic paste, or, for manufacturing external surface coatings, as albuminous substance) can produce exothermic effects within the range 550–650°C.

The most common clay minerals (kaolinite, illite, smectite) are recognizable by their relatively strong endothermic effects within the range 550–650 °C (somewhat higher for chlorite). Carbonates show distinctive endothermic peaks: at 840°C (calcite), and doublets at 780°C and 860°C (dolomite) in static air atmosphere, whose position may vary depending on grain size, crystal size, atmosphere and other concomitant factors [2]. They are due to the escape off CO_2 during the breakdown of their structure (other carbonates are unusual in ancient ceramic materials). Exothermic effects within the range 700–1000°C indicate solid-phase transformations (for example, meta-kaolin into Al-spinell at ca. 980°C).

The presence of these characteristic thermic effects indicates that the primary minerals survived the firing processes required to destroy the structure of the minerals. On the other hand, several peaks may be due to secondary phases (as carbonates, gypsum, salts, etc.). The DTA curves of salts are complex and their interpretation needs familiar experience with the technique, to be coupled with XRD data [3], micro-chemical tests and micro-analyses (scanning electron microscopy and energy dispersive X-ray microanalysis (SEM–EDX)).

The reconstruction of the raw pug mixtures on the basis of the mineralogical association as recognized in the fired bodies is not an easy task, because the original mineralogy could have been deeply modified by the firing techniques; this makes any suggestion as to origin inconsistent [4]. The thermal behaviour of clay minerals and calcite are important for understanding of the reactions occurring during firing. The thermometry of firing processes can be focused on the newly formed phases. The discriminating factor for paragenesis in the ceramic body is the carbonate content (Ca-rich or Ca-poor raw clays). Quartz, feldspars and micas are mainly preserved in

Ca-poor ceramics. Newly formed crystalline phases are not relevant in Ca-poor ceramics within the firing range 700–1000°C. Low amounts of fluxes in Ca-poor raw clays hinder the formation of new phases. Under conditions of equilibrium, the paragenesis of Ca-rich ceramics is generally delimited within the range quartz–anorthite–diopside. K-feldspar generally occurs in less-vitrified bodies. Plagioclase may also be formed during firing, as reaction phase between clay minerals and calcium carbonate (the same is true for diopside).

The decomposition of calcite (in an oxidizing atmosphere) occurs at a lower temperature than for illite. As a consequence, there is free CaO until about 800°C and it can react at higher temperature with clays and SiO_2 forming new silicate phases. In a reducing atmosphere the breakdown of illite and calcite runs almost parallel, and due to increased CO_2 partial pressure, the dissociation of calcite is shifted to higher temperatures (as well as the formation of CaO). Consequently, plagioclase, diopside and gehlenite are also formed later than in an oxidizing firing atmosphere. Haematite is usually present in red firing bodies.

The paragenesis of primary and firing minerals in ancient ceramics and pottery, as recognizable by X-ray diffraction calcareous antiquity, have a particularly stable microstructure over the temperature range of 850–1050°C. The examination of ancient pottery with an analytical SEM is, therefore, valuable for characterizing and distinguishing between the different traditions in ceramic technology in antiquity (because information is obtained on both the extent of vitrification and the firing temperature). The extent of vitrification provides a useful property for characterizing the quality of a pottery, since it influences several microstructural and physical properties which are relevant to its suitability for the various uses to which it might have been put [5].

In the present work DTA, TG–DTG and XRD results from byzantine and medieval ceramics are examined and the derived information on ceramic technologies, concerning raw materials and production conditions are validated by SEM observations, with regard to the extent of vitrification, as well as by the microstructural data provided by porosimetric measurements.

2. Sampling and experimental procedure

Sampling, reported in Table 1, was performed at the ruins of the Great Basilica of Rhodes (6th century); at the Old Fortress of Corfu, at the Martinengo Bastion (16th century) and English barracks (18th century), the English Hospital and the Cavo Sidero Gate; and at the Hagia Sophia Great Basilica of Constantinople (6th–10th century) and the fortification walls (10th century) of Constantinople.

Almost 20 samples were examined by: Mettler 4000 TA, TG 50 analyzer system at a rate of 10°C min^{-1} in a static air atmosphere; Perkin-Elmer thermoanalyzer TG S-2 and DTA 1700 at a rate of 10°C min^{-1} in a static air atmosphere; Siemens D-500, X-ray diffractometer based on an automatic adjustment and analysis system with a Diffract–EVA quality analysis software; scanning electron microscopy (Philips 515), energy dispersive X-ray microanalysis (EDX); and Fisons 4000 porosimeter.

Table 1
Sampling

Sample	Ceramic colour	Location
Venetian Fortress of Corfu		
Corfu 5	Buff	Martinengo bastion
Corfu 15	Red	English barracks, NW wall
Corfu 14	Red	English barracks, W wall
Corfu 20A	Red	Martinengo bastion
Corfu 24	Buff	Martinengo bastion
Corfu 13	Buff	English barracks, E wall
Corfu 23	Buff	English hospital, N wall
Corfu 20B	Buff	Martinengo bastion
Corfu 27	Buff	Cavo sidero gate
Medieval city of Rhodes		
Rhodes 5	Buff	Hatziandreou site
Rhodes 4B	Red	Hatziandreou site
Rhodes 4A	Buff	Hatziandreou site
Rhodes 3	Red	Hatziandreou site
Rhodes 2B	Red	Hatziandreou site
Rhodes 1B	Red	Hatziandreou site
Rhodes 2A	Red	Hatziandreou site
Rhodes 1A	Red	Hatziandreou site
Hagia Sophia in constantinople		
Hagia Sophia Y4	Buff	Hypogenum of Great Basilica
Hagia Sophia Y5	Buff (burried in the ground)	Hypogeum of Great Basilica
Hagia Sophia W2	Red	Byzantine–Ottoman wall of Kons.

3. Results and discussion

The TG results in weight loss % per temperature range are shown in Table 2. The XRD (crystalline phases), the DTA (firing temperatures), the SEM (vitrification extend) results and the microstructural characteristics are shown in Table 3 and expressed as CV (cummulative volume), $P\%$ (percentage porosity), Rm (average pore radius), γ (apparent density) and As (specific surface area). The derived classification of the ceramic categories, according to the profile of the DTG curves, as Ca-rich, Ca-poor and marly clays of intermediate Ca content is validated accordingly.

The **Ca-rich** (Fig. 1) ceramic fragments present a CaO content of over 5% (according to CO_2 weight loss). They show hygroscopic water ~ 2% at about 80°C and some of them intense gypsum peaks at 145°C (samples C5,14). The peaks from 580–640°C show the decomposition of the most common clay minerals (kaolinite, illite, chlorite) recognizable by XRD. Under SEM they register extended vitrification, which is interpreted by the firing temperature in almost all cases at over 850°C. The lower porosity measured is due to the extended glassy phase.

The **Ca-poor** (Fig. 2) characteristic DTG profile, apart from the moisture water (~ 80°C), shows peaks at about 640°C, where clay minerals decomposition occurs.

Table 2
TG–DTG (weight loss per temperature) results

Sample	Weight loss per temperature range (°C)/%					
	< 120	120–200	200–400	400–600	600–650	> 650
Corfu 5	1.1	0.4	0.5	0.7	0.3	5.5
Corfu 15	1.2	3.6	1.7	4.8	0.7	–
Corfu 14	1.2	2.0	1.0	2.0	1.2	8.0
Corfu 20A	2.1	1.0	2.5	5.1	2.5	2.5
Corfu 24	2.3	1.0	1.4	2.5	1.4	–
Corfu 13	0.9	1.6	0.9	1.0	0.6	2.3
Corfu 23	0.9	0.4	1.0	1.9	0.8	1.4
Corfu 20B	3.2	2.3	0.9	2.7	0.7	–
Corfu 27	2.6	0.7	0.9	1.8	0.9	3.7
Rhodes 5	2.8	1.3	1.5	1.8	1.1	6.1
Rhodes 4B	0.8	0.5	0.8	0.7	0.1	0.5
Rhodes 4A	0.9	0.5	0.7	0.5	0.2	0.6
Rhodes 3	1.7	0.8	1.5	1.0	0.9	–
Rhodes 2B	1.5	1.0	1.4	1.5	0.7	3.6
Rhodes 1B	1.3	0.7	1.2	0.9	0.5	3.4
Rhodes 2A	2.8	1.7	2.3	2.8	1.7	8.3
Rhodes 1A	1.5	1.0	1.1	1.5	0.5	2.2
H. Sophia Y4	1.1	0.3	0.6	0.4	0.2	0.5
H. Sophia Y5	1.6	1.2	3.3	0.9	0.3	1.1
H. Sophia W2	1.2	0.6	1.4	1.1	0.3	0.9

Most of the samples present very low firing temperatures (~ 740 °C) and fragmented vitrification at the initial stage. However some exceptions are noted, as in the case of R3 (firing temperature of ~ 800 °C) and in the case of R4B with extensive vitrification and different microstructural characteristics.

The **marly clays of intermediate Ca-content** (Fig. 3) characterizing all the samples from Corfu (C13, 15, 20A, 20B, 23, 24, 27), show intense peaks either of gypsum or of clay mineral composition and variable firing temperatures and microstructural characteristics. It seems that in both cases, i.e. in the Ca-poor and in the marly clays of intermediate Ca content, other discriminating factors should be sought.

According to recent publications the composition and texture of the different calcite and calcium aluminosilicate crystalline phases might explain the difference in vitrification and in behaviour [6]. From the firing temperature assumed (Table 3, DTA results) and SEM micrographs (Fig. 4) an advanced to extensive (Fig. 4b, c) vitrification stage is derived, as far as Ca-rich clays were concerned (C14, 5). Advanced (Fig. 4a) alternates with the initial and fragmented (Fig. 4d, e, f) vitrification stage, according to the absence (C15) or the excess of augite (20A, 20B), respectively, as far as the Ca-poor or the marly clays of intermediate Ca-content are concerned. The key role of CaO transformations is also validated by the fact that when the augite is

Table 3
XRD, DTA (firing temperatures) and SEM (vitrification stage) results, microstructural and physical characteristics

Ceramic/samples colour	Composition (XRD resutls)[a]	Firing temperature (DTA)	Extent of vitrification	Microstructural and physical characteristics (porosimetric data)				
				CV/cm^3 g^{-1}	P/%	Rm/Å	γ/g cm^{-3}	As/m^2 g^{-1}
Ca-rich								
Corfu 5/buff	Q,Au,Cc,An,Do,K,Chl	850	Extensive	0.311	47.27	6224	1.52	4.86
Corfu 14/red	Q,Cc,An,Ab,Gy,Il,Mnt	>850	Advanced	0.152	28.27	995	1.86	6.75
Rhodes 1A/red	Cc,Msc,Q,An	850	Extensive	0.278	42.81	7848	1.54	3.51
Rhodes 1B/red	Q,Cc,An,P1,	960	Extensive	0.134	26.93	3147	2.01	2.24
Rhodes 2A/red	Q,Cc,Msc,An,Amp	850	Extensive	0.149	28.61	1584	1.92	6.81
Rhodes 2B/red	Q,Cc,Msc,An,Amp,Gy	850	Extensive	0.157	29.67	1584	1.89	6.44
Rhodes 5/buff	Q,Msc,An,Cc,Chl	860	Extensive	0.260	40.82	6220	1.57	5.33
Ca-boor								
Rhodes 4A/buff	Q,An,Msc,Au,Amp,Do,Gy	750	Fragmented	0.407	54.54	15254	1.34	1.99
Rhodes 4B/red	Q,Msc,Amp,Cc	730	Extensive	0.143	27.46	3657	1.92	3.84
Rhodes 3/buff	Q,An,Au,Msc,Cc,Do	800	Fragmented	0.303	45.45	9841	1.50	1.76
H. Sophia	Q,An,San,Do,CAH,CSH,Mnt,Cc,K,Msc	740	Initial vitrification					
H. Sophia Y5/buff								
H. Sophia Y4/buff	Q,An,San,Do,CAH,Mt,Cc,K,Msc	740	Initial vitrification					
H. Sophia W2/red	Q,An,San,Do,CAH,Cc	740	Initial vitrification					
Marly clays of intermediate Ca content								
Corfu 13/buff	Q,Cc,An,Ab,Gy,Msc,K	780	Fragmented	0.234	40.25	7757	1.72	1.36
Corfu 15/red	Q,Cc,Do,Sp,Gy,K,Chl	950	Advanced	0.120	22.68	628	1.89	5.37
Corfu 20A/red	Q,An,Cc,An,Do,Chl,K	830	Fragmented	0.152	28.12	6217	1.85	2.68
Corfu 24/buff	Q,Cc,Au,An,Fsp,Msc,Gy	–	Fragmented	0.156	29.48	2500	1.89	8.34
Corfu 23/buff	Q,An,Au,Cc,Do,Gy,K	–	Fragmented	0.264	43.30	4960	1.64	2.01
Corfu 20B/buff	Q,Au,Cc,An	780	Fragmented	0.197	34.87	6217	1.77	3.95

[a] Cc: calcite, Q: quartz, Au: augite, Do: dolomite, Msc: muscovite, An: anorthite, Ab: Albite, Gy: gypsum, Chl: chlorite, Fsp: feldspars, K: kaolinite, Sp: serpentine, I1: illite, Mnt: montmorillonite, Amp: amphibolite, P1: palygorskite, CAH: calcium aluminate hydrate, CSH: calcium silicate hydrate, San: sanidine.

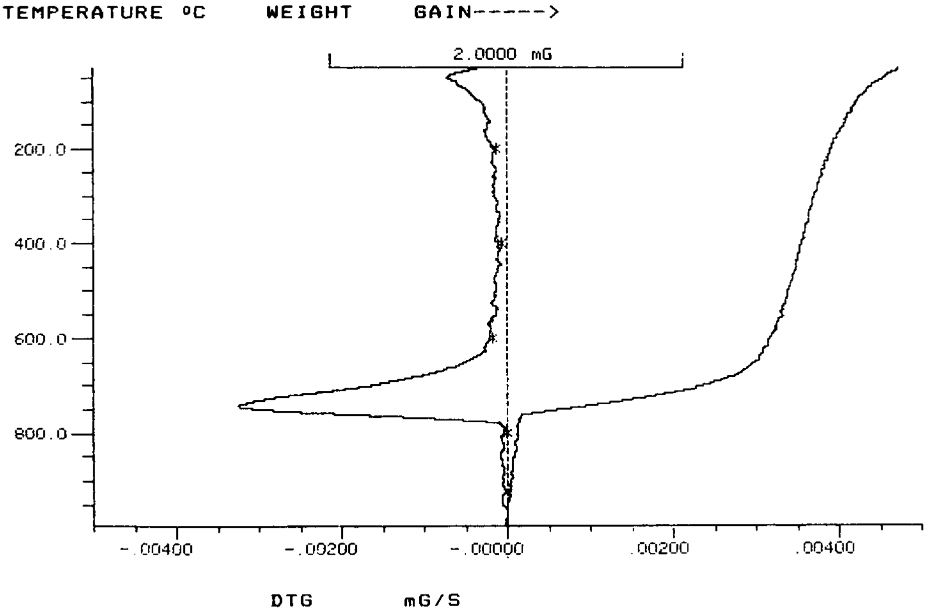

Fig. 1. Ca-rich ceramic.

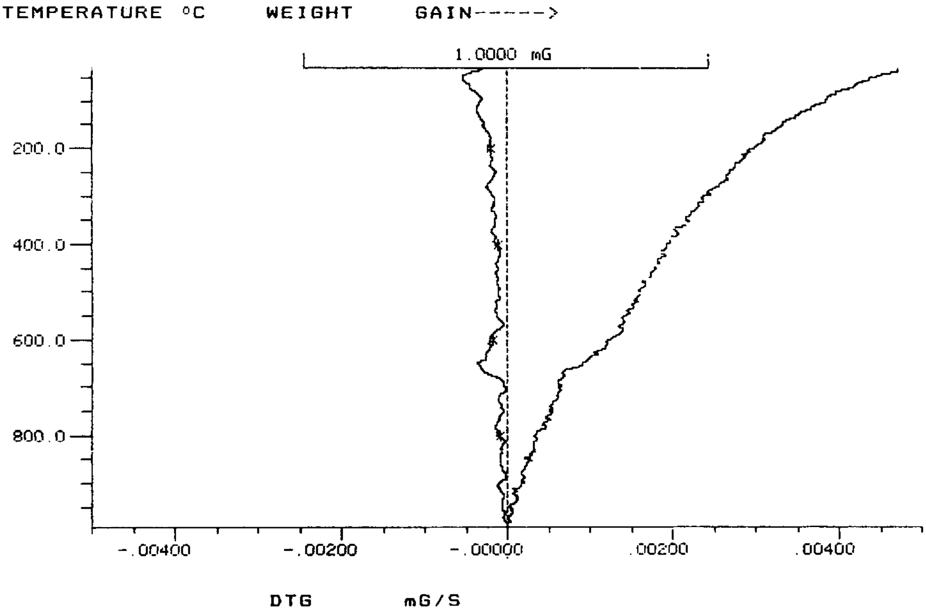

Fig. 2. Ca-poor ceramic.

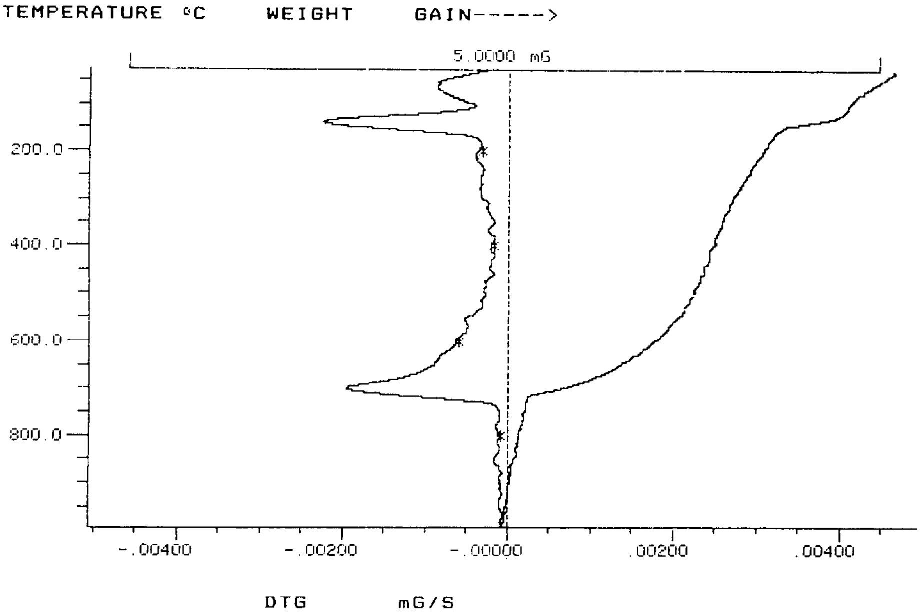

Fig. 3. Marly clay of intermediate Ca content.

present in excess, even in the case of red-coloured ceramics (C20A), initial vitrification is observed.

The alternate presence of augite, anorthite (Table 3, XRD results) gives indications as to the role of CaO transformations in the ceramic matrix. From the two qualities distinguished according to texture and colour, generally, red bricks show extensive vitrification with iron oxide phases dispersed almost homogeneously in the vitreous matrix and buff bricks show fragmented vitrification, where lower concentrations of iron oxides are observed, allocated to large haematite crystals surrounded by lemonite[7]. Even though with slightly different total CaO content, the behaviour of red bricks is governed by the CaO% transformed into the anorthite phase, releasing iron oxides by firing in alternate oxidizing/reducing atmosphere. Buff bricks in contrast, present a higher CaO% transformed into an extended calcium aluminosilicate microcrystalline development, which explains the inhibition and finally the more fragmented vitrification observed, along with the colour difference, due to the trapping of iron in the augite lattice [8]. The resulting texture and vitrification explains the structural and microstructural data. The higher vitrification of the red bricks led to denser, less porous and more durable ceramics [7], as compared to the less vitrified and highly porous buff bricks (Table 3, microstructural data).

However, since paste and temper material seem to be similar for buff and red bricks, different firing conditions within the furnace (i.e. oxidizing and/or reducing atmosphere) should be investigated, as diversifying technological parameters [9].

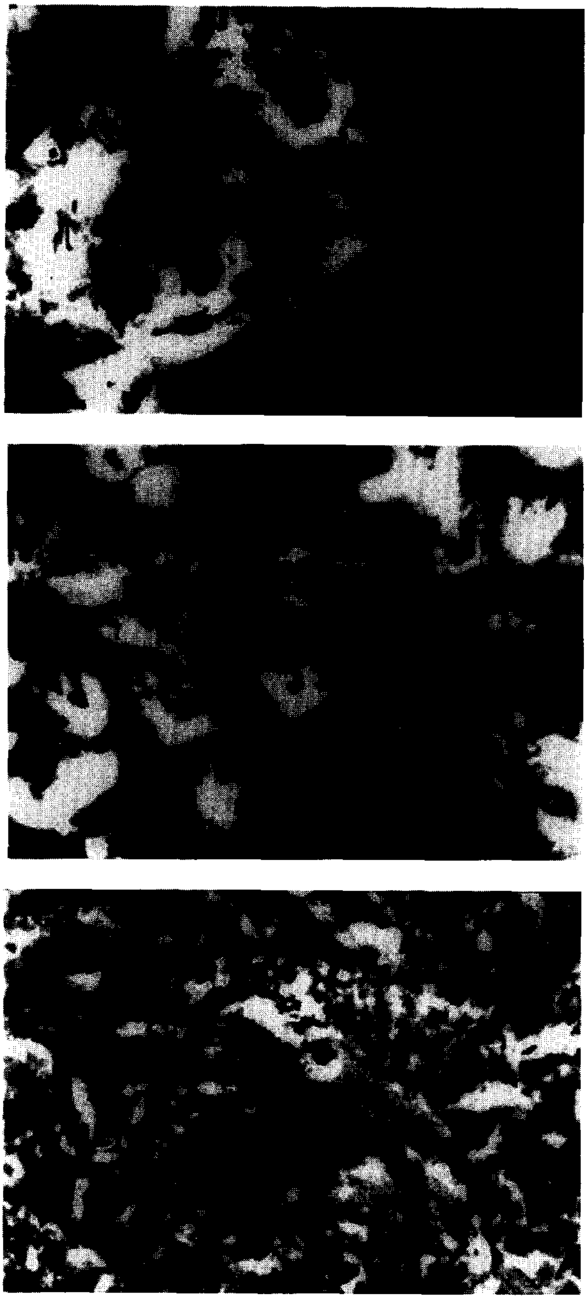

Fig. 4. Characteristic photomicrographs for advanced vitrification (a) (sample C15), extensive vitrification (b,c) (samples C14,5) and fragmented-initial vitrification (d,e,f) (samples C27, 20b, 20a).

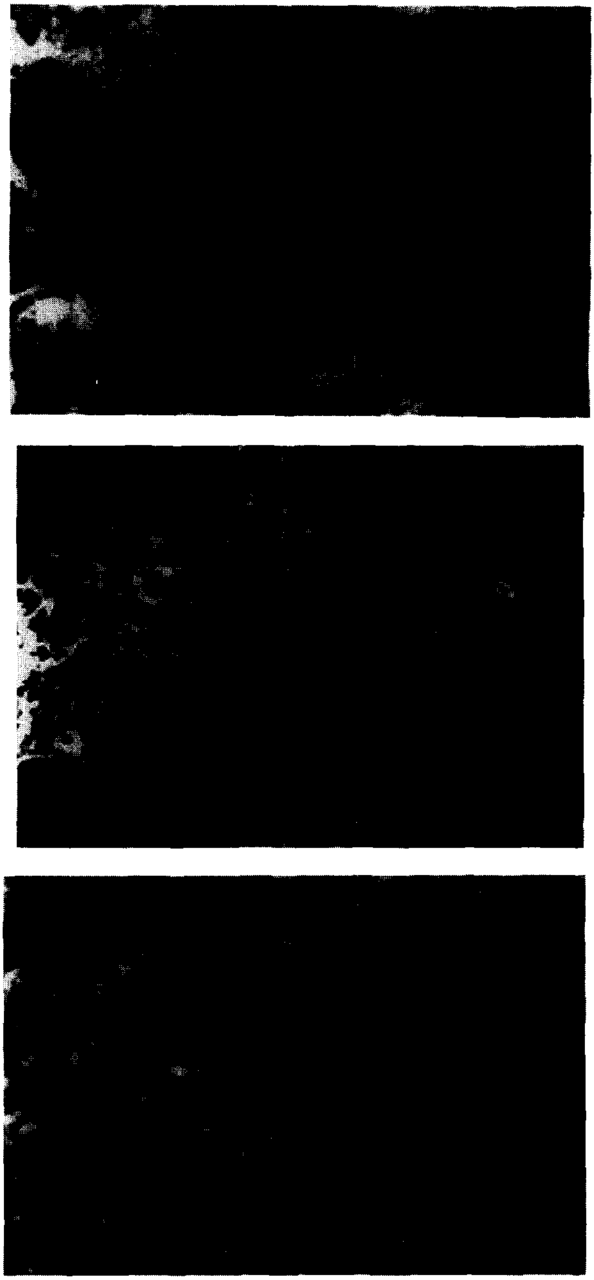

Fig. 4. (*Continued*)

4. Conclusions

Thermal modifications in ceramic microstructure–texture ("fabric") during firing of clay artifacts, are important for appreciating and understanding their manufacturing processes. The nature and development of the ceramic micro-fabric as a function of temperature can also be related to the composition of the clay source exploited. Progressive changes in the body fabric, depending on the increase of firing temperature, can be detected by thin-section petrography and SEM observation.

Ceramic materials represent manufacturing techniques which were improved steadily and consistently over the course of time. The components of ceramic materials are the "fingerprints" of the stable/or metastable solid phase formed during firing and the production processes of antique ceramics and pottery can be derived from their assemblage.

The carbonate content (Ca-rich, Ca-poor or marly clays of intermediate Ca content) discriminates between the paragenesis in the ceramic body, while the type of CaO transformations in the ceramic matrix could inhibit or enhance vitrification according to augite formation.

Acknowledgements

Thanks are expressed to Dr. Y. Maniatis, Demokritos Research Centre and Dr. V. Perdikatsis, IGME and their laboratory colleagues for their kind cooperation.

References

[1] F. Veniale, in Analytical Methodologies for the Investigation of Damaged Stones, advanced workshop, Pavia, Italy, Sept. 1990.

[2] R.C. Mackenzie, in Differential Thermal Analysis 1 and 2, 1st edn., Academic Press, London, 1970.

[3] R.S. Mitchell and S.C. Hart, in R.O. Allen (Ed.), Archaeological Chemistry IV, Am. Chem. Soc., Washington, DC, 1989, pp. 145–155.

[4] Y. Maniatis and S.M. Tite, J. Archeaol. Sci., 8 (1981) 59–76.

[5] F. Sandrolini, G. Moriconi, F. Veniali and G. Zappia, in J.M. Haynes and P. Rossi-Doria (Ed.), Principles and Applications of Pore Structure Characterization, Proc. Int. Symp. RILEM/CNR, Milan, 1993, pp. 291–297.

[6] Y. Maniatis, A. Simopoulos and A. Kostikas, in J.S. Olin and A.D. Franklin (Eds.), Archeaological Ceramics, Smithsonian Institute Press, Washington, DC, 1982, pp. 97–108.

[7] A. Moropoulou, G. Biscontin, P. Theoulakis, K. Bisbikou, E. Zendri, A. Bakolas and P. Maravelaki, in M.J. Thiel (Ed.), Conservation of Stone and Other Materials, Proc. Int. Congr. RILEM/UNESCO, Paris, 1993, pp. 402–410.

[8] A. Moropoulou, P. Theoulakis, K. Bisbikou, J. Rev. des archeologes et historiens d'art de Louvain, 27, 1994.

[9] V. Perdikatsis, Y. Maniatis, A. Simopoulos and A. Kostikas, J. Am. Ceram. Soc., 66 (1983) 773–79.